J. Embryol. exp. Morph. Vol. 33, 2, pp. 419–434, 1975
Printed in Great Britain

Fate maps and the pattern of cell division: a calculation for the chick wing-bud

By J. H. LEWIS[1]

From Department of Biology as Applied to Medicine, The Middlesex Hospital Medical School

SUMMARY

Given the growth rate throughout an embryonic rudiment, one can calculate how its parts must shift as it gets bigger, and so plot fate maps showing their future positions. The calculation is done here for the chick wing-bud from stage 18 to stage 25, using published data for mitotic index and cell packing density, and new measurements of size and shape. Two main findings are: (1) the wing-bud in this period elongates almost uniformly along its proximo-distal axis. (2) Each limb segment derives from the tissue generated by one cell division cycle in the 'progress zone' at the tip.

INTRODUCTION

Different parts of an embryo develop into different parts of the adult. To understand the transformations involved, one must first be able to trace the lineage of each part from start to finish. That is, one must have a set of fate maps. Without knowing what the normal fate of an embryonic tissue would be, one cannot interpret the results of experiments that perturb it: one cannot tell what sort of regulation has occurred.

A traditional way to plot a fate map is to mark patches of embryonic tissue with vital stains or with carbon particles, and so to track down their ultimate positions in the developed organism. In this paper a different method is described: knowing the growth rate throughout an organ rudiment, as indicated, for example, by the mitotic index, one can calculate the trajectory of any part of it, and so trace that part from the embryo to the adult (Fig. 1). For the calculation one requires that there should not be much random cell movement or mixing, and that growth should be predominantly along one axis, so as to allow of one-dimensional analysis. The method is applied to the chick wing-bud, for which these conditions are satisfied (Stark & Searls, 1973).

Fate maps for the chick wing-bud, derived in other ways, have already been published. Saunders (1948) and Amprino & Camosso (1958) have used carbon-particle marking, while Stark & Searls (1973) have used radioactive thymidine labelling to follow the fate of implanted blocks of cells. The carbon-particle

[1] *Author's address:* Department of Biology as Applied to Medicine, The Middlesex Hospital Medical School, London W1P 6DB, U.K.

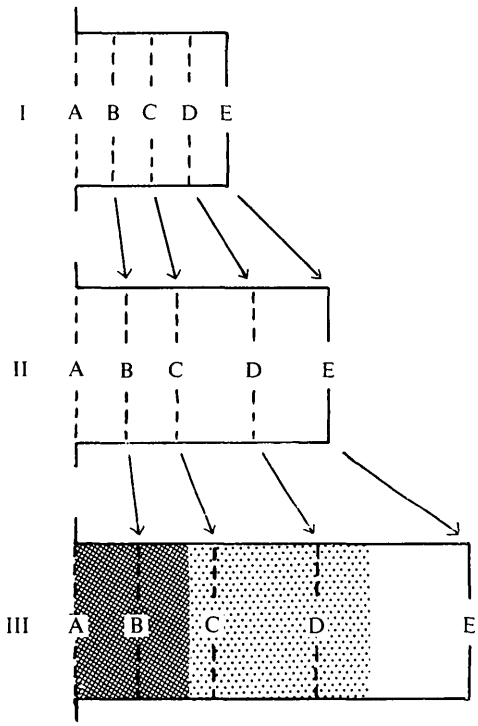

Fig. 1. An idealized outgrowth, elongating along the axis *AE*, is shown at three successive stages, marked I, II and III. Knowing the relative growth rates in the regions *AB*, *BC*, *CD* and *DE* at stage I, one can calculate the new positions to which the cells at *B*, *C* and *D* will have advanced by stage II, and so on for subsequent stages. The calculation is taken as far as a stage where one can by some other means identify the positions of the prospective parts of the adult (indicated by shading at stage III). One can then trace back the positions from which these must have originated at the earlier stages.

method seems to be accurate for the later stages and for the more proximal parts of the limb-bud. But for the distal parts of the early bud it is not reliable. The clusters of carbon particles spread out in the limb mesenchyme and probably shift a little relative to the cells they are supposed to mark. This introduces large errors and uncertainties when applied to the distal parts of early limb-buds, because those parts start small, and are destined to grow and expand by a very large factor. Particles implanted in a single tight cluster may end up scattered over the whole length of a long bone (Amprino & Camosso, 1958; Hampé, 1959). With radioactive labelling, one can at least be confident that the marker does not get separated from the tissue in which it was first incorporated. On the other hand, one cannot be sure how far normal development is disrupted by the grafting of the blocks of radioactive tissue; nor is it easy to locate the grafts accurately in early limb-buds. Thus it seems worthwhile to try to derive a set of fate maps for the early stages by another method, requiring neither surgical interference nor the use of unreliable markers.

I calculate here the displacements of the parts of the wing-bud from stage 18 to stage 25 (Hamburger & Hamilton, 1951), and relate the parts of the stage-25 bud to the parts of the adult wing by means of a fate map of Amprino & Camosso (1958), which is probably reliable for this late stage.

As a by-product, the calculation yields the relationship between the morphological stage of the wing-bud, and the number of division cycles that the mesenchyme cells at its tip have undergone since the beginning of outgrowth. The results imply that, in terms of the progress zone theory (Summerbell, Lewis & Wolpert, 1973; Summerbell & Lewis, 1975), it takes about one division cycle to lay down the rudiment of each bone or row of parallel bones in the limb. This casts an intriguing light on our hypothesis that positional values are assigned by a timing mechanism, and that cell divisions are the ticks of the clock.

MATERIAL AND METHODS

A. *Experiment*

White Leghorn chicken eggs were used; they were incubated at 38 °C and windowed in the usual way after about 3 days of incubation. Data for mitotic index and cell population density in the wing-bud are taken from the papers of Hornbruch & Wolpert (1970) and Summerbell & Wolpert (1972). To find the cross-sectional area of the wing-bud as a function of distance from the tip, two or more embryos were used for each stage from 18 to 25 inclusive. My staging probably conforms to the normal standard (Hamburger & Hamilton, 1951) to within $\pm\frac{1}{2}$ a stage, but may be somewhat less accurate for stage 18. The segment of the trunk carrying the wing-buds was cut out and fixed for at least 2 h in Karnovsky's fixative diluted to half strength, dehydrated through graded alcohols to epoxy propane, and embedded in Araldite. The right wing-bud was mounted for sectioning in a plane perpendicular to its proximo-distal axis, and a Cambridge Huxley-pattern Ultramicrotome Mark I was used to cut 1 μm sections at a succession of distances inwards from the tip.

The interval between sections was measured by the micrometer advance of the knife, to an accuracy of better than $\pm 5\%$. The sections were stained with toluidine blue, and the outline of the mesenchyme was drawn at a fixed magnification on card, using a Wild camera lucida. The card was cut out and weighed, giving a value for the cross-sectional area of the embedded mesenchyme accurate to within about $\pm 5\%$. The total length of limb-bud sectioned, from tip to base, was noted: the base was taken to be the centre of the interface between limb tissue and coelom. The limb-buds had shrunk during fixation and embedding, so that this length was about 30 % less than the length measured *in vivo*. The calculations, however, depend essentially on relative rather than absolute lengths, and so are not upset by shrinkage, if that shrinkage is uniform. The main error probably comes from the difficulty of defining accurately the position of the base of the bud and the alignment of its proximo-distal axis. The

errors are likely to be particularly bad at stage 18, for which the boundary between limb-bud and flank is ill-defined.

B. *Calculation*

Let us consider the displacements of tissue along the proximo-distal axis of outgrowth only; and let x be the distance from the tip along this axis. For each stage S, we need the following data: L_s, the total length from the tip to the base of the bud, i.e. to the coelom; $A_s(x)$, the cross-sectional area of the bud at the level x; $\rho_s(x)$, the mean number of cells per unit volume or 'cell density' at the level x; $\mu_s(x)$, the mean mitotic index at the level x. From these we can work out: $N_s(x)$, the total number of cells within a distance x from the tip, and $R_s(x)$, the total number of new cells created per unit time by mitosis in the population within the distance x from the tip. Specifically

$$N_s(x) = \int_0^x A_s(x')\rho_s(x')\,dx', \tag{1}$$

$$R_s(x) = \int_0^x A_s(x')\rho_s(x')\,\mu_s(x')\frac{1}{m_s}\,dx', \tag{2}$$

where m_s is the duration of the mitotic phase of the cell cycle, and is assumed constant over the limb-bud. The lengths of the other phases of the division cycle, however, and the proportion of cells engaged in the division cycle, may vary: the formula for $R_s(x)$ involves no assumption that they are constant. Let Δt_s be the time interval between stage S and the next stage S'. Let $\Delta N_s(x)$ be the total number of new cells created in the time interval Δt_s by mitosis in the population which at stage S lay within the distance x from the tip. Then provided Δt_s is short compared with the cell cycle time, we have

$$\begin{aligned}\Delta N_s(x) &= R_s(x)\Delta t_s \\ &= \frac{\Delta t_s}{m_s}\int_0^x A_s(x')\rho_s(x')\,\mu_s(x')\,dx'.\end{aligned} \tag{3}$$

The population of $N_s(x)$ cells which filled the region within x from the tip at stage S, will grow by stage S' to a population of $N_{s'}(x')$ cells filling the region within x' from the tip, where

$$N_{s'}(x') = N_s(x) + \Delta N_s(x). \tag{4}$$

We can solve this equation numerically, and so find the new position x' to which the cells at x are displaced during the growth from stage S to stage S'. By repeating the procedure for successive stages, we can trace the fate of the different parts of the limb-bud from the earliest stage in our calculation to the latest. The calculation in this paper is not taken beyond stage 25, since the one-dimensional description begins to break down as the central tissue differentiates into cartilage and becomes more and more different from peripheral tissue in its density and growth rate.

The calculation in practice involves two extra steps. First, since the value of $\Delta t_s/m_s$ is not accurately known from other sources, we deduce it from the increment of the total number of cells in the whole limb-bud, using equations (3) and (4):

$$\frac{\Delta t_s}{m_s} = \left[N_{s'}(L_{s'}) - N_s(L_s)\right]\left[\int_0^{L_s} A_s(x')\rho_s(x')\mu_s(x')\,dx'\right]^{-1}. \tag{5}$$

This makes the final results independent of the absolute value of the mitotic index, and sensitive only to the ratios of the mitotic indices for the different parts of the limb. If, for example, two observers use different criteria to define a mitosis, they will get different absolute values for the mitotic index in each region; but provided the counts of the one bear a constant proportion to the counts of the other (Summerbell, 1973), the calculation will give the same results whichever set of measurements is used.

Secondly, we have to deduce $\rho_s(x)$, the number of cells per unit volume, from counts of $\sigma_s(x)$, the number of cell nuclei per unit area in histological sections. If the nuclei have no preferred orientation and the average nuclear size is independent of the packing density ρ, we have simply

$$\rho_s(x) = c\sigma_s(x), \tag{6}$$

where c is a constant, whose value we do not in fact need to know, since it cancels out of our calculation. But if, for example, the average nuclear volume is inversely proportional to the local cell density, and the effective section thickness is small compared with the nuclear diameter, we have instead

$$\rho_s(x) = c'\sigma_s^{\frac{3}{2}}(x), \tag{7}$$

where c' is again a constant whose value we do not need to know. From Summerbell's (1973) measurements, it seems that equation (7) should be more nearly correct. In any case, I have repeated the whole fate map calculation using the relationships (6) and (7) in turn. The final results differ by only a negligible amount. The results shown in Fig. 4 were calculated assuming equation (7). The calculation is easily done on a computer. A Fortran program was used, involving linear interpolation between the points specified, and integrating by a trapezoidal rule with a step size of 25 μm.

RESULTS

Fate maps

The cross-sectional area $A_s(x)$ of the wing-bud as a function of the distance x from the tip is shown for each stage S from 18 to 25 in Fig. 2*a* and *b*.

Each curve represents the mean of two or more sets of measurements. The variation from specimen to specimen is exemplified in Fig. 3, which shows the individual measurements for four wing-buds all judged to be at stage 24. The measured lengths L_s of the embedded wing-buds are shown in Fig. 4: for the

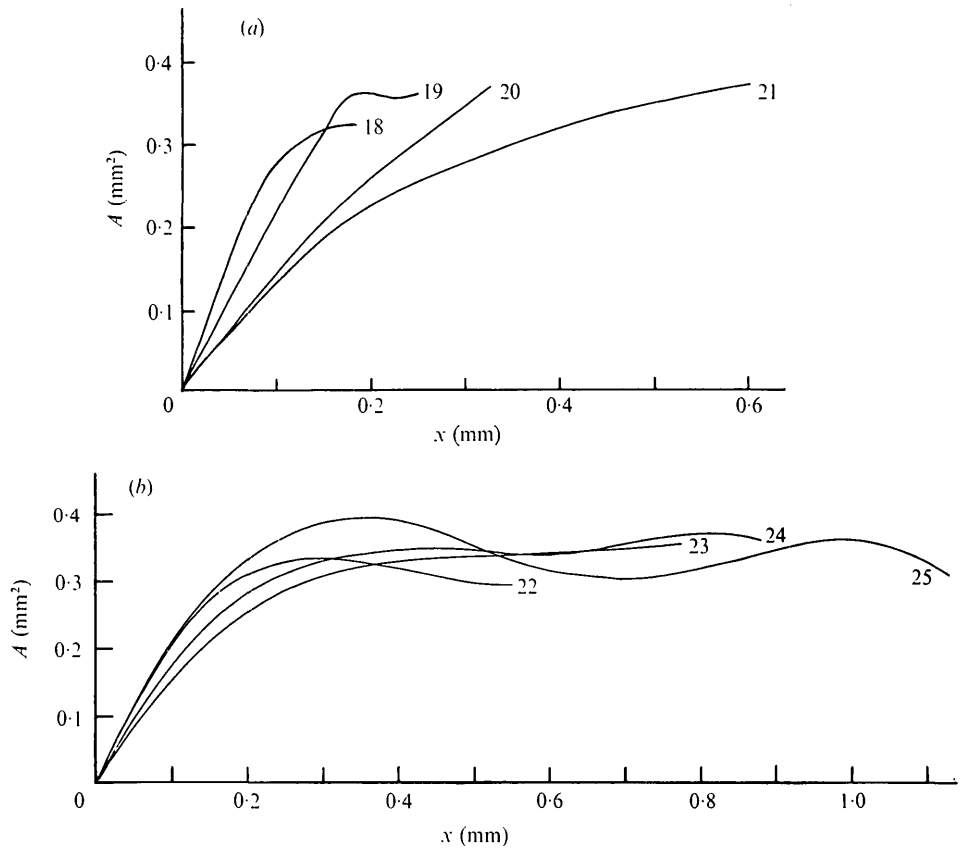

Fig. 2. The cross-sectional area A of the wing-bud, as a function of the distance x from its tip, for each stage from 18 to 25, as marked. Each curve represents an average of the directly measured curves for at least two fixed, embedded specimens.

calculation I took a mean at each stage. Graphs of areal cell density $\sigma_s(x)$ and mitotic index $\mu_s(x)$ can be found in the papers of Summerbell & Wolpert (1972) and Hornbruch & Wolpert (1970). Tables 1, 2, 3, and 4 give the corresponding figures for L_s, $A_s(x)$, $\sigma_s(x)$ and $\mu_s(x)$ that were used in the present computation.

To plot the fate maps, 10 equally-spaced starting points were chosen along the proximo-distal axis of the stage-18 wing-bud. Each of these points may be regarded as the initial position of a particular cell lineage. The subsequent mean positions of each lineage were then calculated as far as stage 25. The results are shown in the right-hand half of Fig. 5. It can be seen that the expansion of the limb is very nearly uniform along its length, throughout the period from stage 18 to 25. The lineage starting half-way along the wing-bud at stage 18 thereafter remains roughly at the mid-point, departing from it in fact by no more than $\pm 5\,\%$ of the length of the bud.

A fate map of Amprino & Camosso (1958) serves to relate the parts of the

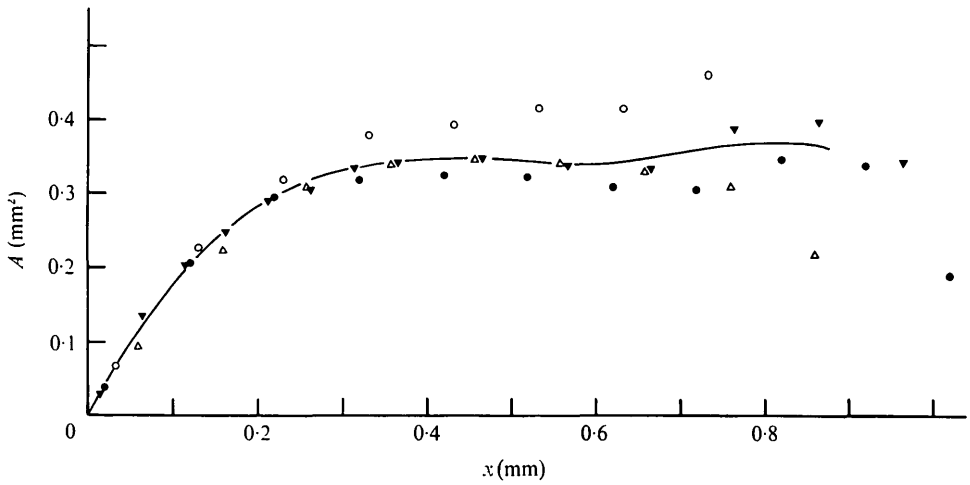

Fig. 3. The cross-sectional area A as a function of the distance x from the tip, for each of 4 specimens (●, △, ▼ and ○), all taken to be at stage 24. The curve represents a mean, judged by eye.

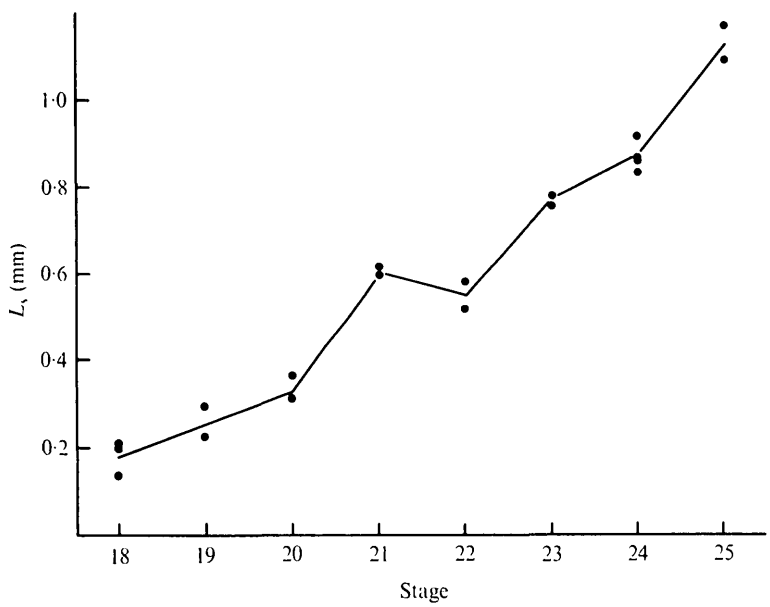

Fig. 4. The measured lengths L_s of individual wing-buds fixed and embedded at different stages S. The line joins the mean values, rounded to the nearest 25 μm, as used in the computation. Note that although the length at what I took to be stage 21 is, perversely, slightly greater than at stage 22, the shape and density are such that the number of cells in the stage-21 bud is slightly less than at stage 22 (see Fig. 6): this suggests that the stage-21 specimens shrank anomalously when fixed and embedded. Mean lengths from flank (not coelom) to tip, as measured *in vivo*, for my stage 19–25 specimens were respectively 275, 375, 650, 800, 1050, 1250 and 1550 μm.

Table 1. *The mean length, L, of a fixed and embedded wing-bud, as a function of stage, S*

Stage, S	18	19	20	21	22	23	24	25
Length, L (μm)	175	250	375	600	550	775	875	1125

Table 2. *The cross-sectional area, A, of the fixed and sectioned wing-bud, as a function of the distance, x, from the tip, and of the stage, S*

Stage, S	Distance from tip, x (μm)									
	0	125	250	375	500	625	750	875	1000	1125
	Area, A (mm^2)									
18	0	0·30	0·30							
19	0	0·27	0·37							
20	0	0·18	0·30	0·41						
21	0	0·17	0·26	0·31	0·35	0·37				
22	0	0·24	0·33	0·32	0·29	0·29				
23	0	0·18	0·29	0·33	0·34	0·34	0·35	0·35		
24	0	0·21	0·31	0·34	0·35	0·34	0·36	0·36		
25	0	0·24	0·36	0·39	0·35	0·31	0·31	0·34	0·36	0·31

Table 3. *The areal cell density, σ, as a function of the distance, x, from the tip, and of the stage, S*

Stage, S	Distance from tip, x (μm)									
	0	125	250	375	500	625	750	875	1000	1125
	Density, σ (cells per 1000 μm^2)									
18	12·3	11·2	11·2							
19	15·8	14·4	13·8							
20	14·8	14·9	15·0	13·8						
21	14·7	16·6	17·0	18·0	15·6	15·6				
22	*16·1*	*17·0*	*17·4*	*18·9*	*18·2*	*17·8*				
23	17·6	17·4	17·8	19·8	20·7	19·9	22·6	22·6		
24	*18·6*	*18·4*	*19·2*	*22·0*	*24·1*	*24·0*	*25·1*	*25·3*		
25	19·7	19·4	20·6	24·3	27·5	28·2	27·7	28·0	27·5	27·5

From Summerbell & Wolpert (1972). Gaps in their data are filled in by linear interpolation (italicized).

stage-25 bud to the parts of the adult limb. Since the wing-bud outline that they draw for stage 24 corresponds more closely to what people in this laboratory judge to be the Hamburger–Hamilton stage 25 than does their stage 25, I adopt their stage-24 fate map as my stage-25 fate map, and use it together with the right-hand half of Fig. 5 to trace back the origins of the adult parts to early

Table 4. *The percentage of cells in mitosis, μ, as a function of the distance, x, from the tip, and of the stage, S*

	Distance from tip, x (μm)									
Stage, S	0	125	250	375	500	625	750	875	1000	1125
	Mitotic index, μ (%)									
18	12·1	12·3	12·5							
19	12·4	11·5	10·7							
20	9·5	8·7	8·5	8·1						
21	7·1	6·7	7·5	8·1	7·1	5·4				
22	*6·5*	*6·2*	*7·7*	*7·7*	*6·3*	*5·2*				
23	5·9	5·7	7·9	7·3	5·5	5·0	4·8	4·3		
24	*6·6*	*6·2*	*6·7*	*6·0*	*4·8*	*4·4*	*4·3*	*4·1*		
25	7·2	6·8	5·6	4·7	4·2	3·8	3·8	4·0	3·6	3·6

From Hornbruch & Wolpert (1970). Gaps in their data are filled in by linear interpolation (italicized).

stages. The results are shown in the left-hand half of Fig. 5. It should be emphasized that, in the present essentially one-dimensional calculation, the curvature of the boundaries between limb territories off the main proximo-distal axis of the bud remains uncertain. In Fig. 5, following Amprino & Camosso, I draw the boundaries somewhat arbitrarily as straight lines orthogonal to the main axis.

Population growth and the cell cycle count

The computer program prints out, among other things, the total number of cells in the wing-bud at each stage, divided by a certain constant, K, of the order of unity. (The exact value of K, for present purposes, does not matter; assuming a mean nuclear diameter of 6 μm (Summerbell, 1973), I estimate roughly that $K = 4$.) The numbers printed out are graphed on a logarithmic scale in Fig. 6. It can be seen that, for example, the number of cells in the stage-25 wing-bud is 14·0 times as great as in the stage 19, corresponding to 3·8 population doublings. Setting aside the rather unreliable results for stage 18, the calculated number of cells at any stage is probably not in error by more than about ± 30 %, so that the figure of 3·8 population doublings between stages 19 and 25 is probably accurate to within about $\pm 0{\cdot}7$.

From the fate map calculations, one can also deduce the number of doublings undergone by specific parts of the whole population, and in particular by the cells near the tip of the wing-bud, that is, in the progress zone (Summerbell *et al.* 1973; Summerbell & Lewis, 1975). At stage 25, there are calculated to be 61 000K mesenchyme cells within 300 μm of the tip, where K is the constant mentioned above. Tracing their lineage back, one finds that they derive from the 1700K cells within 51 μm of the tip at stage 18, the numbers at intermediate stages

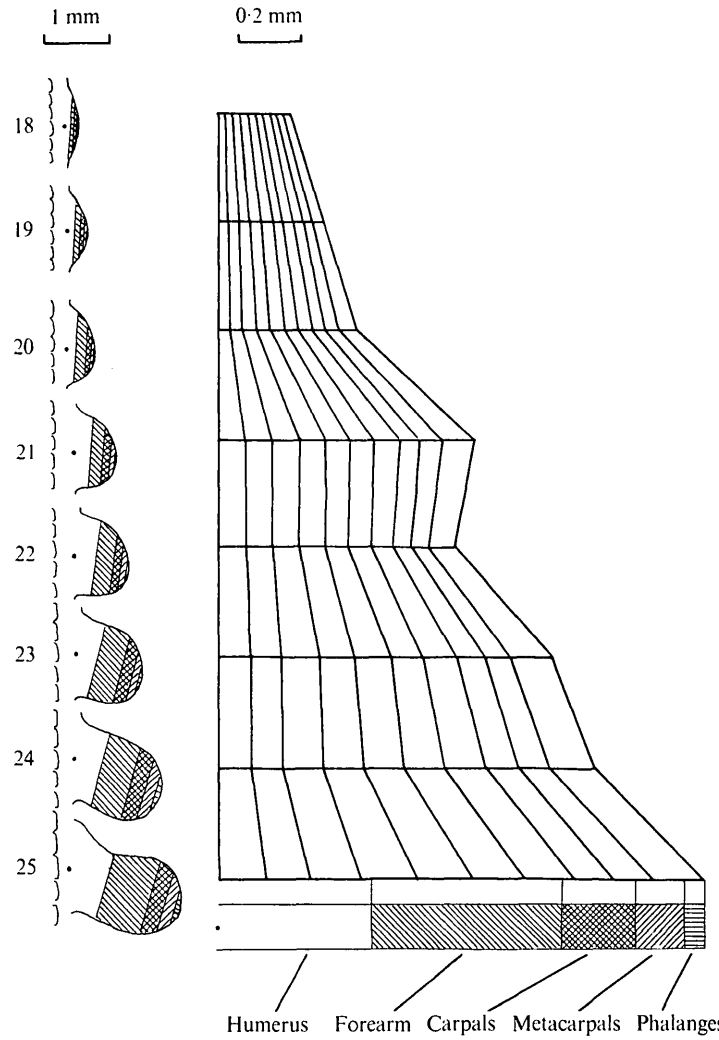

Fig. 5. In the right-hand half of the figure, each horizontal line represents the proximo-distal axis of a wing-bud at the stage specified. (The scale is corrected by a uniform factor for shrinkage.) The downward lines show the displacements of the cell lineages from one stage to the next. The strip at the bottom shows the correspondence at stage 25 with the parts of the adult, according to the fate map of Amprino & Camosso (1958). The trajectories of those parts are hence traced back to the earlier stages, giving the fate maps shown on the wing-bud outlines on the left. In transferring the calculated results onto these standard *in vivo* dorsal views, I scale down the stage-21 axis, as though allowing for anomalous shrinkage (see legend to Fig. 4).

being shown in Fig. 7. The number of times this sub-population doubles, from stage 18, is indicated on the same graph. Since, according to our observations, there is practically no cell death in the mesenchyme at the tip of the wing-bud, and all the cells there are actively dividing (Summerbell & Lewis, 1975), one may equate the number of population doublings with the number of cell cycles.

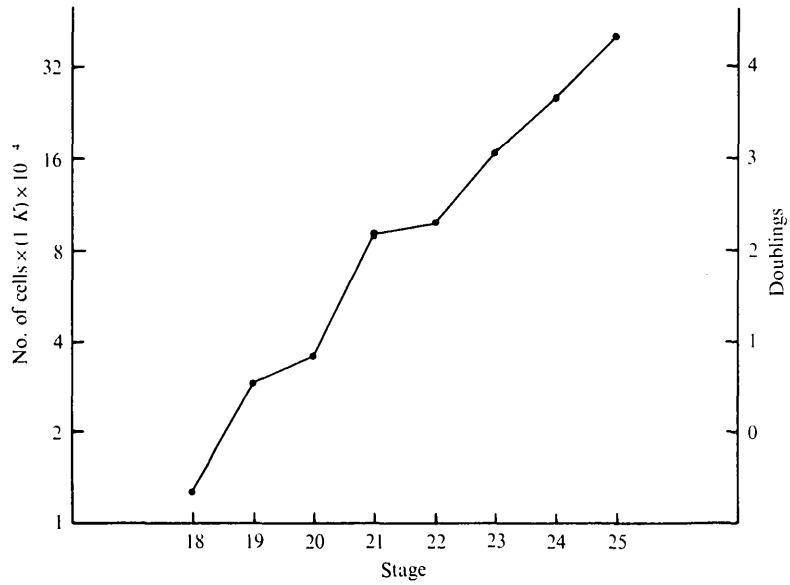

Fig. 6. The total number of cells in the wing-bud as a function of stage. The ordinate axis on the right gives the number of population doublings that have occurred.

This gives directly the number of cell cycles which elapse at the tip of the limb-bud from stage 18 onwards as far as stage 25. This is the number which we have elsewhere called the *age* of the limb-bud, τ (Summerbell & Lewis, 1975). One can easily extrapolate to somewhat later stages, as follows. From stage 22 up to stage 27, and probably some way beyond, the mitotic index of the mesenchyme at the tip stays roughly constant at 6·5(±0·7) %, and the time per stage stays roughly constant at 8 h (Hornbruch & Wolpert, 1970; Hamburger & Hamilton, 1951). The number of cell cycles per stage should therefore also be roughly constant, assuming that the constancy of the mitotic index implies constancy of the cell cycle time. One can therefore make a simple linear extrapolation of the age-versus-stage graph, based on its gradient in the region from stage 22 to stage 25, as shown in Fig. 7. The same straight line provides a good fit also to the points calculated for the earlier stages; throughout the period of limb development which concerns us, 1 division cycle of the tip mesenchyme corresponds to very nearly 1·5 Hamburger–Hamilton stages. No point on the graph departs by more than ±0·8 of a stage from this linear relationship. For general purposes, the age-versus-stage relationship is probably best read off from the fitted straight line, which represents a way of smoothing out idiosyncrasies in my staging.

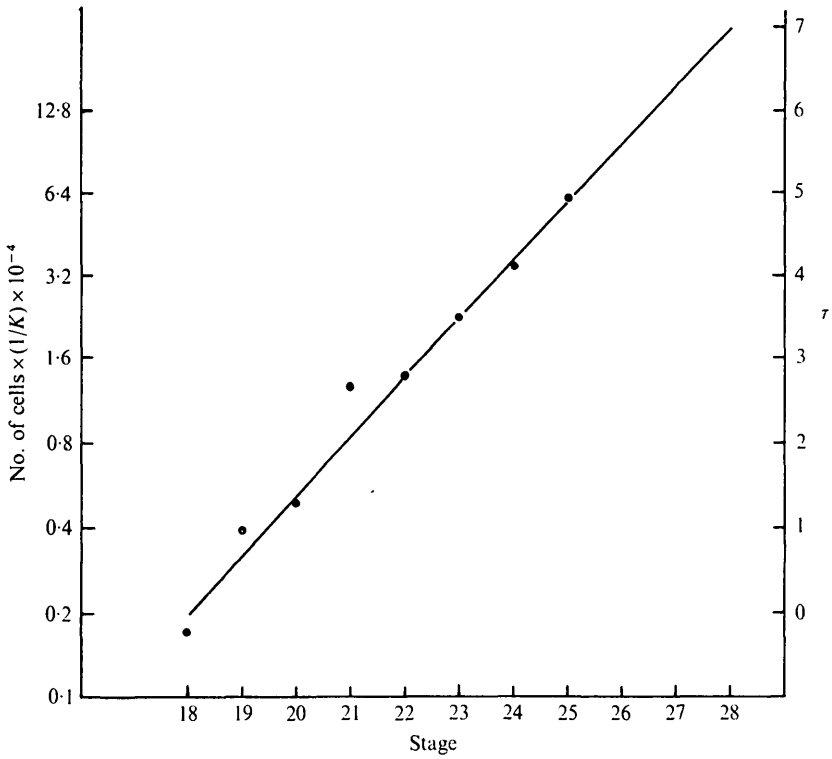

Fig. 7. Cell proliferation at the tip of the wing-bud. The left-hand ordinate gives for each stage the number of cells ancestral to those within 300 μm of the tip at stage 25. The right-hand ordinate gives the corresponding number of population doublings and hence of cell division cycles at the tip since about stage 18; this is the age of the wing-bud, τ. The significance of the fitted straight line is explained in the text.

DISCUSSION

Fate maps for the chick wing-bud

As far as the proximal parts are concerned, there is fairly good agreement between the fate maps worked out here and those of Saunders (1948), of Amprino & Camosso (1958), and of Stark & Searls (1973). The discrepancies concern the distal parts. The wrist and hand, for example, simply are not represented in the fate maps of Saunders for stages 19 and earlier, or in those of Amprino & Camosso for stages 21 and earlier; this reflects the inadequate resolving power of the carbon-particle marker method. Stark & Searls, using tritiated thymidine labelling, are able to plot the presumptive digits even at the earliest stages; but they allot practically no space on their fate maps to the presumptive carpals. By contrast, the fate maps calculated here follow Amprino & Camosso (1958) in showing the presumptive carpal region as a much larger fraction of the early wing-bud than it is of the adult wing. There is evidence from other sources that the early rudiment of the carpal region is indeed disprc-

portionately large. The change in its relative size depends on changes of cell population density and proliferation rate. By about stage 31, the cells in the wrist are packed together to about twice the mean number per unit volume found in the forearm and metacarpal regions on either side, and the dilution of tritiated thymidine label shows that since stage 24 they have undergone on average about one division cycle less than the cells in those adjacent segments (J. Lewis, unpublished observations). From whole mounts stained with alcian green at the intervening stages, it can be seen directly that while the forearm increases its length by a factor of 4 or 5, the rudiment of the wrist barely grows at all (Wolpert, Lewis & Summerbell, 1974). From these whole mounts, it looks as though even the fate map borrowed here from Amprino & Camosso for stage 25 may allot too little space to the carpals, placing the boundary between them and the forearm about 100 μm too close to the tip.

Apical ridge removal provides further evidence of the peculiarity of the wrist rudiment (Summerbell, 1974). There is a period of about 4 stages during which that operation always gives a limb truncated through the wrist, implying that the rudiment of the wrist takes about twice as long as the rudiment of a long bone to be laid down by the progress zone mechanism.

The cell cycle time in the chick wing-bud

There do not seem to be any other published estimates of the relation between the Hamburger–Hamilton stage and the age of the wing-bud measured in cell division cycles at its tip. The cell cycle time has, however, been measured by Cairns (1966) and by Janners & Searls (1970), using tritiated thymidine. Their values can be compared with the present estimate that one cell cycle at the tip lasts 1·5 Hamburger–Hamilton stages. According to Janners & Searls, the stage length increases from about 4 h at stage 19 to about 8 h at stage 24. Thus 1·5 stages at stage 19 equals about 6 h, and at stage 24 about 12 h. Cairns (1966) finds the cell cycle time to range between roughly 6 and 8 h from stage 19 to stage 23. Janners & Searls (1970), however, find the cycle time to be almost twice as long: 13·5 h at stage 19 near the tip of the bud and 13·2 h at stage 24 there. But these latter figures may be overestimates if, as we have suggested elsewhere (Summerbell & Lewis, 1975), Janners & Searls underestimate the labelling index in their experiments. I have in fact repeated a few of Janners & Searls' continuous labelling measurements, and get consistently higher values for the labelling index (J. Lewis, unpublished observations). My measurements, however, like those of Janners & Searls, show a wide scatter, perhaps because of local fluctuations of growth rate within the limb-bud. This makes it difficult to deduce an accurate value for the cell cycle time by the continuous labelling method. It is noteworthy that whereas Janners and Searls find the cell cycle time near the tip to be slightly *longer* at stage 19 than at stage 24, Hornbruch & Wolpert (1970) find the mitotic index there to be almost twice as high as at stage 24, implying that the cycle time is much *shorter* at stage 19 than at stage 24.

Taking all these results together, the fate map calculation seems to give estimates of the relation between the stage and the cell cycle count that agree tolerably well with independent data on cell cycle times.

Cell cycles, limb segments, and the progress zone theory

According to our progress zone theory (Summerbell *et al.* 1973; Summerbell & Lewis, 1975), the patterning of the limb depends on a timing mechanism. The parts are laid down in proximo-distal succession by proliferation of the cells in a 'progress zone' at the tip of the limb-bud; and they emerge from that zone equipped with 'positional values' which govern their subsequent growth and differentation into the appropriate bones, muscles, etc. The positional value of each cell may directly determine its behaviour, so that differentiation outside the progress zone is cell-autonomous; or, perhaps more probably, the local mean positional value may specify the parameters of some later short-range cell-cell interactions which thereby generate in each region the appropriate histological details. The positional value is itself determined by the time which has been spent in the progress zone; the tissue which comes out very early forms the proximal part of the humerus, and the tissue which comes out very late forms the tips of the digits. We have suggested that the measure of time in the progress zone, by which the positional value is established, may be the number of division cycles undergone there. Now the stage at which each part of the limb emerges from the progress zone can be estimated from the results of apical ectodermal ridge removal (Summerbell, 1974). Fig. 7 then gives for each stage the corresponding number of cell division cycles that have elapsed at the tip of the bud (see Summerbell & Lewis, 1975, fig. 5). Within the limits of experimental error, the results fit the hypothesis that each skeletal element, or row of parallel skeletal elements, corresponds to an interval of one cell cycle. As explained above, we may regard the wrist of the chick as equivalent to about two such limb segments, represented by two rather ill-defined rows of embryonic carpals. The chick wing then comprises 7 segments: upper arm, forearm, carpals I, carpals II, metacarpals, phalanges I, phalanges II. These are laid down between stage 18 and stage 28; and between stage 18 and stage 28, according to Fig. 7, about seven cell division cycles elapse at the tip of the limb-bud.

Thus the quasi-periodic pattern of the limb, with its alternation of bones and joints, may be somehow correlated with the periodicity of cell division. A positional value established by counting division cycles may serve to modulate the repetition, so that each segment grows and develops in a distinctive fashion. The underlying mechanisms are as yet obscure; it should be emphasized that the cells do not appear to divide in synchrony either in the progress zone or elsewhere in the limb-bud.

General applicability of the method

The method presented here for calculating fate maps has two virtues: it does not require the use of markers, which may wander or fade, and it does not depend on surgical interference. Instead, the necessary data on cell numbers and mitotic index can all be gathered from sections of the fixed entire organ rudiment. Thus the method should be especially valuable for small and inaccessible structures, such as the imaginal discs of insects. The resolution attainable is not limited by the magnification of a dissecting microscope or the clumsiness of micro-surgery. Thus the fate maps given here for the chick wing-bud show the origins of the most distal parts even at very early stages, whereas carbon-particle fate maps have left these something of a mystery. In fact, the present maps approach the irreducible limit of resolution for any fate map, set by the amount of random cell movement and mixing (Lewis, Summerbell & Wolpert, 1972). The extent to which this blurs the boundaries between presumptive territories is discussed elsewhere (Lewis, 1973).

The calculation depends on certain assumptions – for example, that the duration of the mitotic phase is constant. This should ideally be checked. The most serious limitation of the method is, however, geometrical: the analysis is basically one-dimensional. It becomes much more difficult if the rate and direction of growth vary according to the position along other axes besides the main axis of outgrowth. Systems undergoing complicated distortions, such as the avian blastoderm or the amphibian gastrula, would present problems. On the other hand, the method could easily be applied to structures with a high degree of symmetry, such as plant meristems, or the retina, where outgrowth is radial.

It may sometimes be a long dull job to gather the data for the calculations (especially if there are no published measurements available already). On the other hand, one can extract a lot of useful and detailed information besides the fate maps themselves. In this paper, for example, it has been possible to relate the morphological stage to the age measured in cell division cycles in a particular region. The findings cast a faint but fresh light on the mechanism by which an anatomical pattern is laid down in a growing embryo.

I thank Lewis Wolpert, Dennis Summerbell, Margaret Goodman and the Science Research Council for guidance, comments, practical help and money.

REFERENCES

AMPRINO, R. & CAMOSSO, M. (1958). Analisi sperimentale dello sviluppo dell' ala nell' embrione di pollo. *Wilhelm Roux Arch. EntwMech. Org.* **150**, 509–541.

CAIRNS, J. M. (1966). Cell generation times and the growth of the chick wing bud. *Am. Zool.* **6**, 328.

HAMBURGER, V. & HAMILTON, H. L. (1951). A series of normal stages in the development of the chick embryo. *J. Morph.* **88**, 49–92.

HAMPÉ, A. (1959). Contribution a l'étude du développement et de la régulation des déficiences et des excédents dans la patte de l'embryon de poulet. *Archs. Anat. microsc. Morph. exp.* **48**, 345–478.

HORNBRUCH, A. & WOLPERT, L. (1970). Cell division in the early growth and morphogenesis of the chick limb. *Nature, Lond.* **226**, 764–766.

JANNERS, M. Y. & SEARLS, R. L. (1970). Changes in rate of cellular proliferation during the differentiation of cartilage and muscle in the mesenchyme of the embryonic chick wing. *Devl Biol.* **23**, 136–165.

LEWIS, J. (1973). The theory of clonal mixing during growth. *J. theor. Biol.* **39**, 47–54.

LEWIS, J. H., SUMMERBELL, D. & WOLPERT, L. (1972). Chimaeras and cell lineage in development. *Nature, Lond.* **239**, 276–279.

SAUNDERS, J. W. (1948). The proximo-distal sequence of origin of the parts of the chick wing and the role of the ectoderm. *J. exp. Zool.* **108**, 363–403.

STARK, R. J. & SEARLS, R. L. (1973). A description of chick wing bud development and a model of limb morphogenesis. *Devl Biol.* **33**, 138–153.

SUMMERBELL, D. (1973). *Growth and regulation in the development of the chick limb.* Ph.D. thesis. University of London.

SUMMERBELL, D. (1974). A quantitative analysis of the effect of excision of the AER from the chick limb-bud. *J. Embryol. exp. Morph.* **32**, 651–660.

SUMMERBELL, D. & LEWIS, J. H. (1975). Time, place and positional value in the chick limb-bud. *J. Embryol. exp. Morph.* **33**. (In the Press.)

SUMMERBELL, D., LEWIS, J. H. & WOLPERT, L. (1973). Positional information in chick limb morphogenesis. *Nature, Lond.* **244**, 492–496.

SUMMERBELL, D. & WOLPERT, L. (1972). Cell density and cell division in the early morphogenesis of the chick wing. *Nature New Biol.* **238**, 24–26.

WOLPERT, L., LEWIS, J. H. & SUMMERBELL, D. (1974). Morphogenesis of the vertebrate limb. In *Cell Patterning*. London: Ciba Foundation – Elsevier (in the Press).

(Received 24 July 1974)